Q-SLOPE ANALYSIS OF NIOBIUM SC RF CAVITIES

K.Saito #, KEK, 1-1 Oho, Tsukuba-shi, Ibaraki-ken, Japan

Abstract

Q-slopes, which usually appear in the Qo-Eacc excitation curve of superconducting RF niobium cavities, are analysed by two models: global heating model and magnetic penetration model. Qo-Eacc excitation curves are nicely fitted by the combination of these models.

Q-SLOPES

Since the discovery of baking effect of niobium bulk superconducting (sc) RF cavities [1], one has much interest in Q-slopes appeared in the Qo-Eacc excitation curves. Usually one observes three kinds of Q-slope. These Q-slopes are typically seen in electropolished and none baked cavities as shown in Fig.1. In Fig.1, Q-slop III is related to the bake effect. When one takes baking for instance 2 days at 120°C during vacuum evacuation, the Q-dropping disappears and the high gradient often goes up to 40MV/m [2]. J.Halbritter et al. [3] explains this effect as oxygen diffusion from the oxygen contaminated surface into the bulk. The similar Q-slope appears in chemically polished cavities too, but the bake effect is much less by previous experiments [2]. J.Knobloch et al. have related the Q-slope III to the magnetic field enhancement at grain boundary steps on electron beam welding seam of equator section in niobium cavities [4]. He simulated the local heating due to breaking of superconducting state by the field enhancement.

So far, however there is no explanation based on characteristic of superconductivity about these Q-slopes. The author proposes here a simple model, which can explain both Q-slope II and III by the BCS scheme.

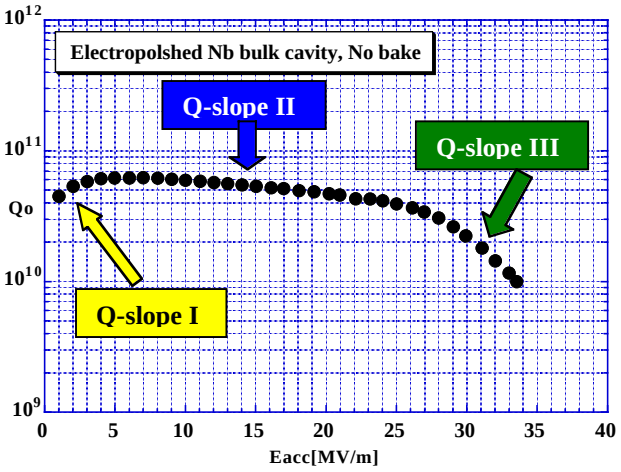

Figure 1: Q-slopes observed in Q-Eacc excitation curves of sc niobium cavities electropolished and no baked.

This model handles the combination of global heating due to the poor thermal conductivity of superconductors and RF magnetic field penetration effect, which reduces the band gap with increased RF field. These both effects bring the field dependent surface resistance increase. That results in the Q-slopes. The Q-slope I is also observed in many laboratories but it is out of scope in this paper.

GLOBAL HEATING MODEL

At first, as an easy explanation for both Q-slopes: II and III, global heating might be considered. The author analysed Qo-Eacc excitation curves and developed that only this model is insufficient to explain the Q-slope III.

Surface Resistance and Qo-value

Surface resistance of sc cavities is calculated by BCS theory:

$$R_{BCS}(T) = C \cdot \frac{\omega^2}{T} \cdot \exp(-\frac{\Delta}{k_B T}) \quad (1),$$

here k_B is Boltzmann constant, T cooling temperature, C a constant depended on the material, ω the angular frequency of the microwave. Δ is the band gap and related to the transition temperature (T_C) of the superconductivity by BCS theory:

$$2 \cdot \Delta(0) = 3.52 \cdot T_c \quad (2).$$

While experimental surface resistance is well fitted by the formula:

$$R_S(T) = R_{BCS}(T) + Rres \quad (3).$$

Here, Rres is a constant and is called as residual surface resistance. In Fig.2 shows the measurement result of temperature dependence of the surface resistance. It is obtained by a nearly defect free cavity of 1300 MHz (JL-1), which achieved Eacc=40 MV/m with no field emission (no X-ray). Data of Fig2 were obtained at low field: ~ 3MV/m. The result was fitted by Eq.(3):

$$R_S(T) = \frac{A}{T} \cdot \exp(-\frac{B}{T}) + R_{res} = \frac{1.13E-4}{T} \cdot \exp(-\frac{18.7}{T}) + 1.01E-8 \quad (4).$$

These fitting parameters: A, B and Rres are used in the later Q-slope analysis. On the other hand, Rs is related to Qo by the so called geometrical factor **Γ**:

$$Qo = \frac{\Gamma}{R_S} \quad (5).$$

ksaito@post.kek.jp

Γ is 274 in our 1300 MHz single cell cavities, which is used in the later Q-slope analysis.

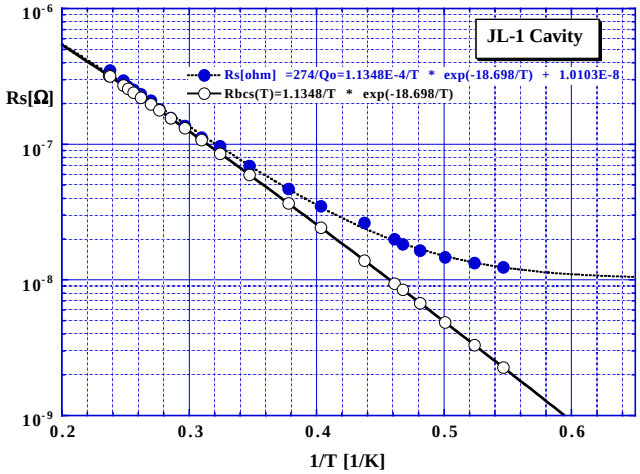

Figure 2: Temperature dependence of surface resistance of nearly defect-free cavity (JL-1).

Thermal Conductivity in SC State

In sc state, thermal conductivity (κ_S) is very small because electrons in the Cooper pare have no contribution to heat transfer. Bellow the λ-point of liquid helium, most of electrons condense to the Cooper pair. κ_S depends on the niobium material for instance RRR. Here, we handle the sc niobium cavities with RRR=200. We calculated the temperature dependence of κ_S with RRR=200 niobium material using the formula in the reference [5]:

$$\kappa_s(T) = R(y)\cdot\left[\frac{\rho_{295K}}{L\cdot RRR\cdot T} + a\cdot T^2\right]^{-1} + \left[\frac{1}{D\cdot\exp(y)\cdot T^2} + \frac{1}{BlT^3}\right]^{-1} \quad (6),$$

$$L = 2.05E-8,\ RRR = 200,\ \rho_{295K} = 14.5E-8\ \Omega m,\ a = 7.52E-7$$

$$-y = \alpha\cdot\frac{T_c}{T},\ \alpha = 1.53,\ T_c = 9.25K,\ T = 1\sim 4.25K$$

$$D = 4.27E-3,\ B = 4.34E3,\ l = 50\mu m$$

here the R(y)-function is the ratio of electron conductivity between sc state and normal conducting state. The notation is given in the reference [6]:

$$R(y) = \frac{\kappa_{es}}{\kappa_{en}} = \frac{2F_1(-y) + 2y\ln(1+e^{-y}) + \frac{y^2}{(1+e^y)}}{2F_1(0)}, \quad (7).$$

$$F_n(-y) = \int_0^\infty \frac{z^n}{1+e^{z+y}}dz$$

Fermi-Dirac function: $F_n(-y)$ is tabulated by Rhodes [7] up to –y=4.0 but we need here the values for more larger –y because of the lower cooling temperature: 1.3 ~ 2.2K. For such larger –y value, we used a fitting function instead of direct integration of Eq.(7) as shown in Fig.3:

$$F_1(-y) = 0.87222\cdot\exp(-0.95932y) \quad (8).$$

This fitting function is not good for small –y for instance $F_1(0)$=0.8224670 in Rhodes calculation but is expected very good for the larger –y=6.43(2.2K) ~ 10.9(1.3K). Using these results, we calculated κ_S and fitted by the following formula as seen in Fig. 4:

$$\kappa_{RRR=200}(T) = -4.0697 + 10.462\cdot T - 9.2994\cdot T^2 + 3.0024\cdot T^3 - 0.12441\cdot T^4 \quad (9).$$

Around 1.5K, where we usually measure sc cavities at KEK, one notices κ_S is only 0.2W/(**K**·**m**). The temperature dependence is very sharp. κ_S changes one order of magnitude between 1.5K and 2.2K.

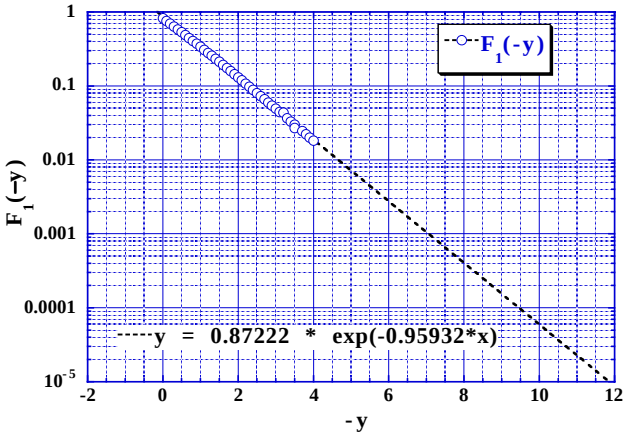

Figure 3: Extrapolated curve with F_1(-y) function for larger –y.

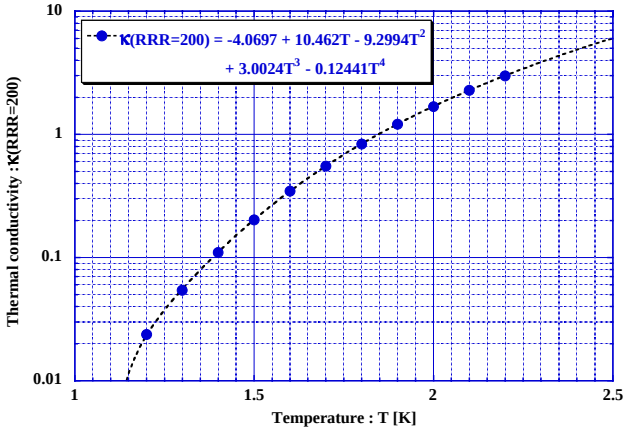

Figure 4: Temperature dependence of κ_S for RRR=200.

Kapitza conductance

In addition to the poor thermal conductivity of sc niobium material, Kapitza thermal resistance h_k makes smaller the thermal conductivity between the outer surface of the cavity and face of the liquid helium. For niobium one can find out the measurement results in the reference [8]. We fitted the data as:

$$h_k(T) = 705.51\cdot T^{3.7113} \quad (10).$$

The fitting is shown in Fig.5.

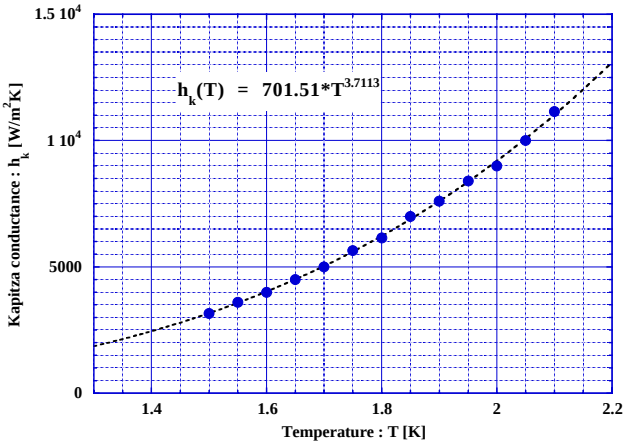

Figure 5: Temperature dependence of Kapitza conductance.

Effective Heating Area

When we calculate heat flux (q), we need the heating surface area. We define the effective heating surface area (S_{eff}) with dissipated loss (P_{loss}) as:

$$P_{loss} = \frac{1}{2} R_s \int_s H_s^2 dS = \frac{1}{2} R_s \cdot H_p^2 \cdot S_{eff} \qquad (11),$$

here H_P is the surface peak magnetic field. In our cavity geometry, S_{eff} = 0.0878m^2 and is about 75% of the whole cell surface. Heat flux is calculated from the S_{eff} in the one dimensional model as:

$$q = \frac{P_{loss}}{S_{eff}} \qquad (12).$$

Global Heating

Now, the preparation has finished for the global heating model. At low field, the RF surface temperature should be same as the bath temperature (T_b), however, at high field, it becomes higher by ΔT due to the poor thermal conductivity in the cavity wall. This temperature difference is calculated using q, κ_S and h_k as following:

$$\Delta T = q \cdot \left\{ \frac{d}{\kappa_S(\tilde{T})} + \frac{1}{h_k(\tilde{T})} \right\} \qquad (13),$$

here d is the cavity wall thickness and 2.2~2.3mm in our case. $\tilde{T}$ is the cavity temperature and defined by the RF surface temperature (T) and the bath temperature as:

$$\tilde{T} = \frac{T_s + T_b}{2} = T_b + \frac{\Delta T}{2} \qquad (14).$$

In addition, Ts is written as:

$$T_s = T_b + \Delta T \qquad (15).$$

When the temperature difference ΔT happens on the RF surface, Ts becomes higher with increased RF fields due to the larger heat flux. BCS surface resistance is very sensitive for the RF surface temperature as Eq.(1), and the temperature increases quickly RF surface resistance Thus Q-slope might happen through the feedback loop as Eq. (16).

$$T_S = T_b + \Delta T: \quad \Delta T \Rightarrow \Delta R_{BCS} \Rightarrow \Delta T \quad (\Uparrow \Leftarrow \Downarrow) \qquad (16).$$

Now let's see how this theory can reproduce the Q-slope in a nearly defect free case (JL-1 cavity). The Qo-Eacc excitation curve is presented in Fig.6. The result had no field emission: no x-rays. We have two ways to calculate the RF surface temperature. One is to calculate Eq.(15) and the other is to evaluate the Ts directly from the Qo-Eacc curve by graphic solution using Eqs.(4) and (5). Eq.(4) offers a good temperature sensor. At first, we calculate the Ts by the graphic calculation. From the Qo-Eacc excitation curve in Fig.6, one calculates R_S(Eacc):

$$R_S(Eacc) = \frac{\Gamma}{Q_o(Eacc)} = \frac{274}{Q_o(Eacc)} \qquad (17).$$

Then one sets Rs(Eacc) = Eq.(4):

$$R_s(Eacc) = \frac{A}{T_s} \cdot \exp(-\frac{B}{T_s}) + R_{res} \qquad (18).$$

Eq.(18) can be solved graphically and one gets Ts(Eacc) for each gradient. The result is present in Fig.7. One will notice that the Ts increases linearly with Eacc over a wide range and it is not a quadric increase with Eacc as expected from Eq.(13). The meaning will be explained later. Anyway, this result requires setting Eq. (15) as following:

$$T_s = T_b + \Delta T = T_b + C \cdot Eacc = 1.554 + 0.0158 \cdot Eacc \qquad (19).$$

To see the consistency of the data analysis, we input Eq.(19) into Eq.(4) and calculate Qo:

$$Q_0(Eacc) = \frac{274}{\frac{1.13E-4}{1.554+0.0158 \cdot E_{acc}} \cdot \exp(-\frac{18.7}{1.554+0.0158 \cdot E_{acc}}) + 1.01E-8} \qquad (20).$$

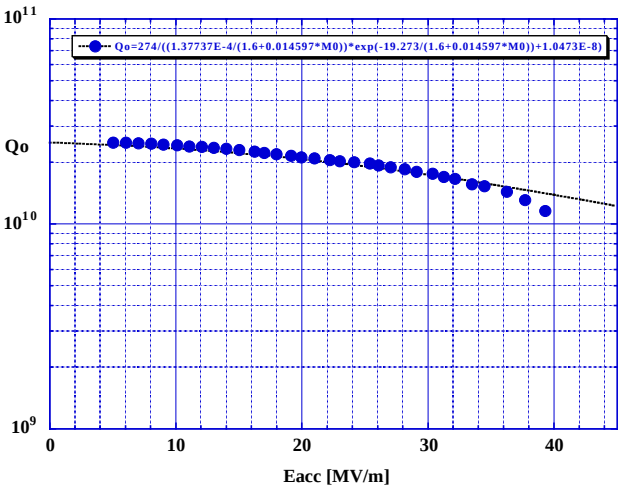

Figure 6: Qo-Eacc excitation curve with the nearly defect-free cavity.

The result is presented in Fig.6 by dotted line. The Qo-Eacc excitation curve is well reproduced by this analysis except for the high gradient region of Eacc > 33MV/m.

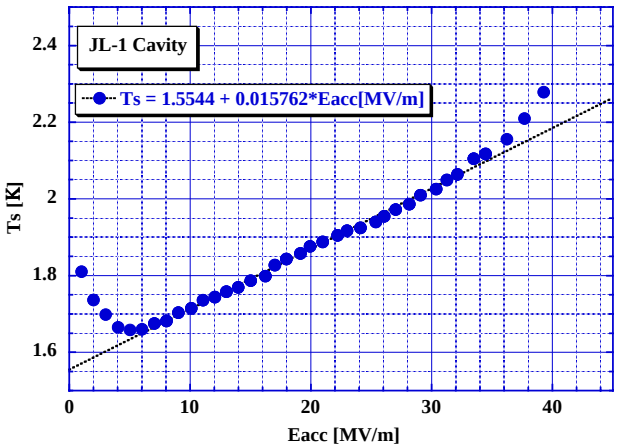

Figure. 7: Temperature increase on the RF surface in the Qo-Eacc excitation curve (nearly defect-free case).

In the next, let's calculate the Ts from Eqs.(13) and (14). This method is a little bit complicated. It needs an iterated calculation. At first, we suppose that RF surface temperature at low field for instance 1.01 MV/m is the same as the bath temperature. One calculates $\kappa_S(0)$ and $h_k(0)$ setting $Ts=T_b=1.735$ K by Eqs.(9) and (10). Then inputting these values and d=2.3 mm into Eq.(13), one calculates $\Delta T(1)$, $\tilde{T}(1)$ and Ts(1) by Eqs.(14) and (15). In addition, inputting $\kappa_S(1)$ and $h_k(1)$ into Eq.(13), we calculate $\Delta T(2)$, $\tilde{T}(2)$ and Ts(2). One iterates the similar calculation for next i:

$$\Delta T(i) = q(i) \cdot \left[\frac{d}{\kappa_S(i-1)} + \frac{1}{h_k(i-1)} \right].$$

The calculation result is tabulated in Table 1. In Fig. 8, the result is plotted for T_b and Ts from the graphic solution of Qo(Eacc). The calculated Ts in this iteration reproduces the Ts by the graphical method within an error

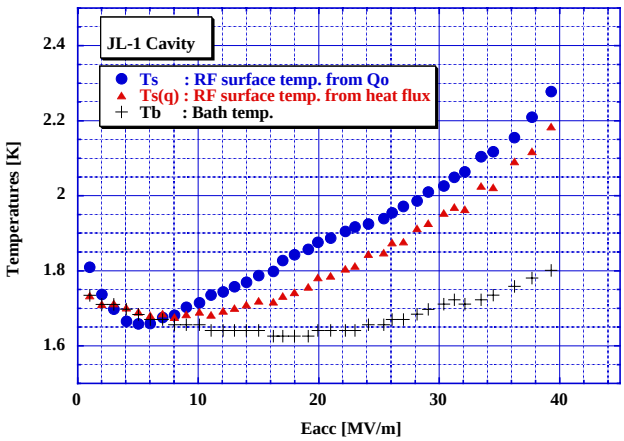

Figure 8: The RF surface temperature calculated from heat flux and bath temperature.

Table 1: Iterated calculation results of RF surface temperature

No	Eacc(i)	q(i)	$T_b(i)$	$\kappa_S(i)$	$h_k(i)$	$\tilde{T}$ (i)	Ts(i)
1	1.01	0.074	1.735	0.641	5319	1.735	1.735
2	2.01	0.283	1.711	0.641	5319	1.711	1.712
3	3.01	0.617	1.711	0.579	5066	1.712	1.713
4	4.05	1.095	1.698	0.581	5074	1.700	1.702
5	5.04	1.693	1.684	0.552	4950	1.687	1.691
6	6.04	2.431	1.670	0.522	4823	1.676	1.682
7	7.04	3.336	1.670	0.496	4711	1.679	1.687
8	8.04	4.366	1.656	0.502	4736	1.667	1.677
9	9.03	5.566	1.656	0.475	4619	1.670	1.684
10	10.10	7.017	1.656	0.483	4654	1.674	1.691
11	11.07	8.546	1.641	0.490	4687	1.662	1.683
12	12.07	10.215	1.641	0.465	4577	1.667	1.694
13	13.01	11.984	1.641	0.476	4626	1.671	1.701
14	14.01	14.023	1.641	0.485	4663	1.676	1.710
15	15.03	16.356	1.641	0.495	4707	1.681	1.720
16	16.24	19.443	1.626	0.506	4756	1.672	1.718
17	17.03	21.746	1.626	0.487	4670	1.679	1.733
18	17.99	24.633	1.626	0.504	4744	1.685	1.743
19	19.15	28.300	1.626	0.515	4795	1.692	1.758
20	19.95	31.309	1.641	0.532	4867	1.712	1.783
21	21.00	35.122	1.641	0.582	5076	1.714	1.787
22	22.22	40.069	1.641	0.587	5097	1.724	1.805
23	23.01	43.563	1.641	0.612	5199	1.727	1.813
24	24.13	48.361	1.656	0.621	5239	1.751	1.845
25	25.39	54.495	1.656	0.685	5498	1.753	1.849
26	26.09	58.613	1.670	0.692	5524	1.773	1.876
27	27.04	64.356	1.670	0.751	5759	1.774	1.879
28	28.10	71.152	1.685	0.755	5776	1.799	1.914
29	29.09	78.422	1.697	0.833	6080	1.812	1.927
30	30.38	87.479	1.711	0.876	6246	1.833	1.955
31	31.27	95.900	1.723	0.948	6521	1.847	1.970
32	32.14	103.50	1.711	0.998	6709	1.838	1.965
33	33.49	119.73	1.723	0.965	6587	1.875	2.026
34	34.48	129.49	1.735	1.105	7111	1.879	2.023
35	36.24	152.31	1.759	1.123	7175	1.925	2.092
36	37.70	180.82	1.781	1.319	7896	1.950	2.119
37	39.29	222.00	1.801	1.432	8306	1.993	2.185

0.05~0.1K. In addition, the linear dependence with Eacc at middle fields is well reproduced by this method too. The linear temperature increase is the result of the sharp temperature dependence of κ_S. Heat flux increases in quadric with Eacc and increases ΔT. The temperature becomes higher, while the thermal conductivity also increases at the same time. This effect is against the ΔT increase and results in the linear increase. It is worthwhile to see the difference between Rs(Qo(Eacc)): from graphical calculation and Rs(Ts(q)): from flux calculation in Fig.9. The result is presented in Figs.9 and 10. A field dependent difference is seen. This suggests an unknown loss mechanism is included in Rs(Qo). From these analysis we summarized as following:

1) Global heating requires the RF surface temperature increase linearly with increased Eacc.
1) This model can reproduce rather well the Q-slope II over the wide range of Eacc but does not fit the high gradient region (Q-slope III).
1) It is suggested that Rs(Qo) still includes a hidden loss mechanism.

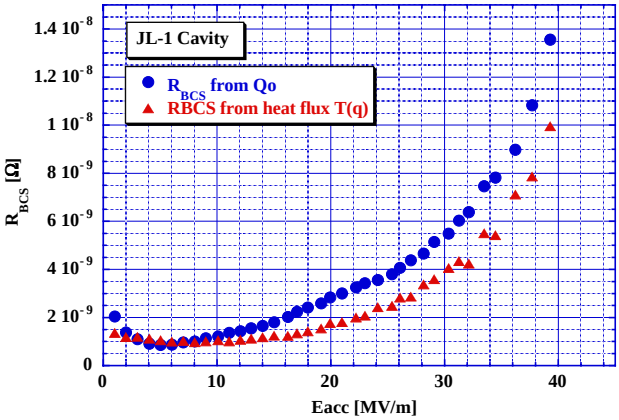

Figure 9: Comparison of the Rs(Qo(Eacc) and Rs(T(q)).

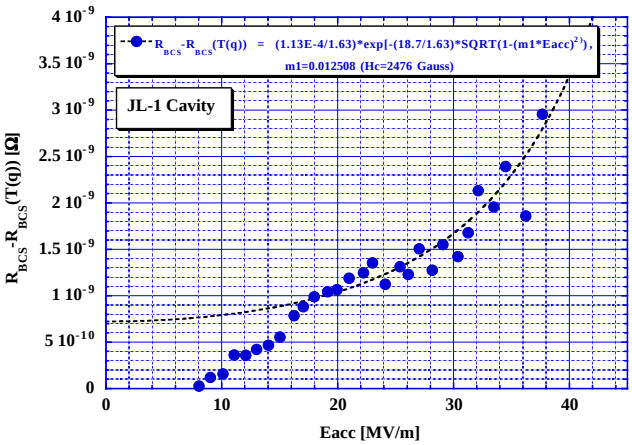

Figure 10: A field dependent difference between Rs(Qo(Eacc)) and Rs(Ts(q)).

MAGNETIC FIELD PENETRATION MODEL

Here, we propose the magnetic field penetration model as the unknown effect in Rs(Qo). It might be a question from theoretical point of view. Really superconductor has the Meissner effect and expels perfectly the external magnetic field. However, one should remind that this is not true for the RF cavity measurement, which picks up the characteristics only of the skin depth of the niobium with a high sensitivity.

The effect of the external magnetic field (parallel to the surface) on the energy gap of superconductors, which is the boundary effect of λ / d (λ: penetration depth, d: thickness of the specimen), is known on the film superconductors: aluminium and lead with several 1000 Angstroms [9]. The gap of the 3000 Angstroms thick aluminum has the second order transition, while 4000 angstroms thicker aluminum film has the first order transition. The author supposes the second order like transition for the field penetration about the unknown effect in the Qo-Eacc excitation curve. Then, the field dependent energy gap will be given as:

$$\Delta(H) = 1.76 \cdot \Delta(0) \cdot \sqrt{1 - \left(\frac{H}{H_C}\right)^2} \qquad (21),$$

here H_C is the thermo-dynamical critical magnetic field of the niobium. Whether this assumption is right or not will be entrust to the result of the later analysis. As seen later, this assumption leads to the same result as expected from the bulk property if the skin has no field enhancement and has the normal H_C value as the bulk. When we input Eq.(21) into the formula of BCS surface resistance Eq.(1), we have to remind to use the effective RF magnetic field($H/\sqrt{2}$). The magnetic surface peak Hp can be used instead of H. Thus, Eq(4) is re-written as:

$$R_s(T_B, Eacc) = \frac{A}{T_B + C \cdot Eacc} \cdot \exp\left[-\frac{B \cdot \sqrt{1 - \left(\frac{H_p}{\sqrt{2} \cdot H_c}\right)^2}}{T_B + C \cdot Eacc} \right] + R_{res} \qquad (22),$$

$$H_P = \alpha \cdot Eacc$$

$$Q_o(T_b, Eacc) = \frac{\Gamma}{R_{BCS}(T_b, Eacc) + Rres} \quad ,$$

here the global heating is included. The parameters: A, B and Rres in Eq.(22) are obtained independently by measurement of the temperature dependence of Rs at low field. Eq.(22) is essentially two parameters fitting with a Qo-Eacc curve. In Fig.10 the difference Rs(Qo(Eacc))-Rs(Ts(q)) is fitted with Hc=2476 Gauss:

$$R_s(Qo(Eacc)) - R_s(T(q)) \approx \frac{A}{T_B} \cdot \exp\left(-\frac{B \cdot \sqrt{1 - \left(\frac{H_p}{\sqrt{2} \cdot H_c}\right)^2}}{T_B} \right) \qquad (23).$$

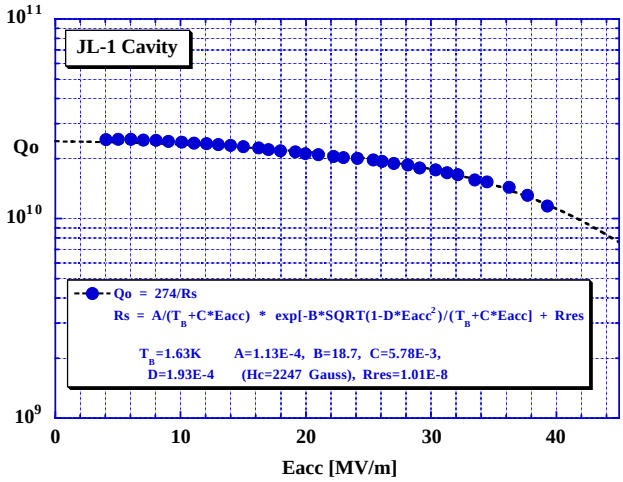

Figure 11: Fitting result by the combination of the global heating and magnetic field penetration model for the Qo-Eacc excitation curve in nearly defect-free cavity.

The number of H_C is too large by 24% but within the analysis error.

Now let's see how this model fits the Q-slopes. Fig.11 is a fitting result by the parameters. A, B and Rres are fixed by the numbers in Eq.(8). Only C and H_C are free parameters in the fitting. The fitting results are C=3.78E-3, H_C=2247 Gauss. The H_C value is 10% high but reasonable within analysis error. The Qo-Eacc excitation curve is reproduced very nicely including the high gradient region by the combination of the global heating and this model.

OTHER Q-SLOPE ANALYSIS

Chemically Polished Cavity

Let's make the same analysis for a chemically polished and baked cavity. The RRR of the cavity is 230. The RF surface temperature evaluated in the Qo-Eacc excitation curve is presented by the mark ■ in Fig.12. Though it is no discussed in this paper, up to 7MV/m the apparent temperature decrease is observed due to the Q-slope I in spite of the constant bath temperature (+). Up to 20MV/m, a linear temperature increase (T_S(Qo(Eacc)): RF surface temp.) with increased Eacc is observed. The other temperatures calculated from the heat flux (q) presented, i.e. RF surface temperature Ts(q)(●), cavity temperature Tc(q)(▲) are also plotted in Fig.12.

Fig 13 shows the comparison between the BCS surface resistance and that calculated from the heat flux. Fig. 14 shows the different of these surface resistances. It can be fitted by Eq. (14) with H_C=945 Gauss and C=4.46E-3. Of course, other parameters are fixed the values from the Rs temperature dependence measurement around 3 MV/m: A=1.71E-4 ΩK, B=18.7. Rres=5nΩ,.

Fig.15 is the fitting result of the Qo-Eacc excitation curve by the combination of the global heating and the magnetic penetration model. In this case, H_C and C were free parameters and other parameters were fixed to the above numbers. The fitted values are H_C=984.3 Gauss and C=4.46E-3 K/[MV/m].

This cavity was baked at 120^{O}C for 48 hours after the chemical polishing but the Q-slope did not disappear. The lower H_C value might come from the field enhancement due to the rough surface by CP, i.e. if there happens the field enhancement the inside term in the square root in the Eq.(22) has to be replaced by:

$$\sqrt{1-\left(\frac{\beta H_p}{\sqrt{2}H'_c}\right)^2}$$

here β is the field enhancement factor. Then, the parameter fitting result by Eq.(22) is:

$$H_c = \frac{H'_c}{\beta} \qquad (24).$$

The fitted value is small by $1/\beta$ ($\beta > 1$) from the real critical field (H'_c).

This cavity achieved 40 MV/m in the later experiment by electropolishing and the Q-Eacc excitation curve was fitted with H_C=2200 Gauss. Thus the ratio: 2200/984=2.3 is the field enhancement value. This number is consistent with Knobloch's simulation result [4].

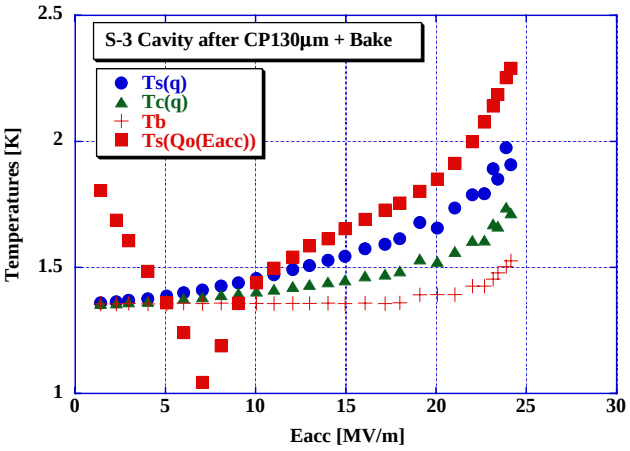

Figure 12: Temperatures of the chemically polished and baked cavity.

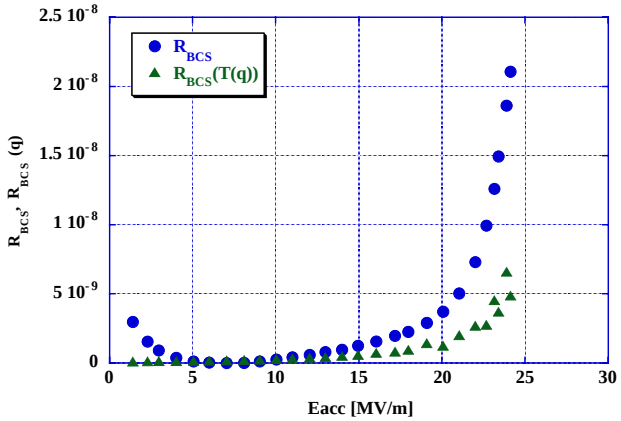

Figure 13：Comparison between the R_{BCS} calculated from Qo and the R_{BCS} from heat flux.

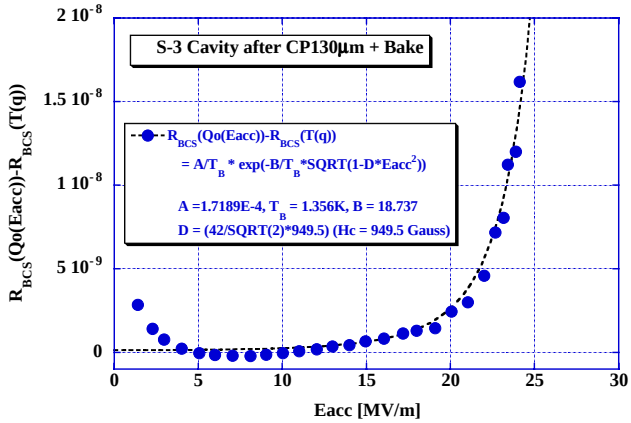

Figure 14: Fitting of R_{BCS}(Qo(Eacc))-R_{BCS}(T(q)) by the magnetic penetration model.

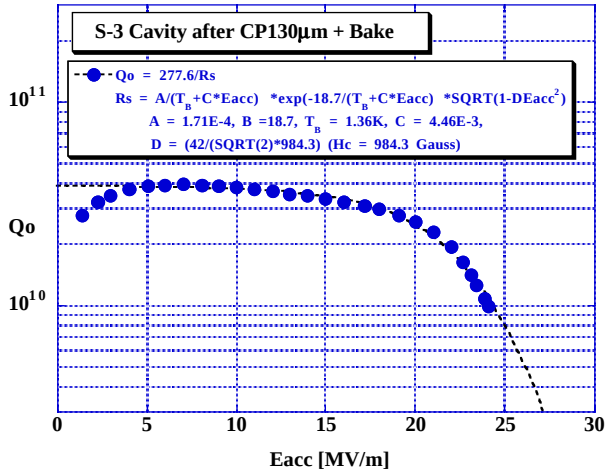

Figure 15: Q-slope analysis by the magnetic field penetration model with a chemically polished cavity.

Electropolished and None Baked Cavity

For the case: electropolished and none baked cavity, the result is presented in Fig.16 by the combined model. In this case, the nice fitting is obtained with H_C=1454 Gauss and C=6.76E-3. The other parameters are fixed the values from the Rs (T) measurement around 3 MV/m: A=1.26E-4, B=18.4, Rres=4.6 nΩ. The surface roughness will be smooth enough because of electropolishing and have less influence on the field enhancement. Therefore, the lower H_C value will be due to the oxygen contamination.

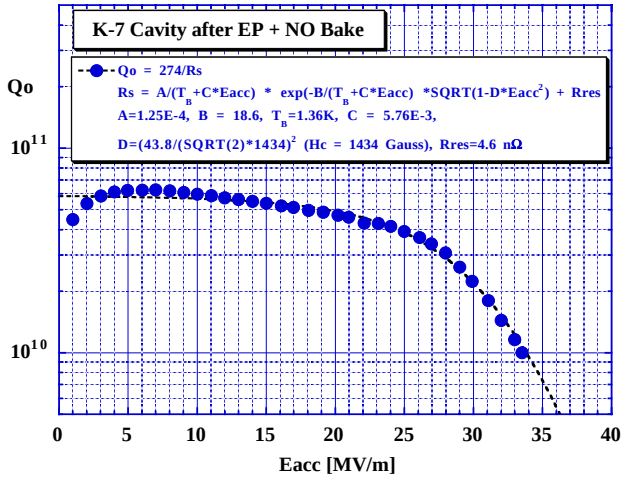

Figure 16: Q-slope analysis with electropolished and no baked cavity.

Ozonated Water Rinsed Cavity

In the above analysis, the oxygen contamination suggests the lower H_C. Concerning to that, the ozonated water rinsed cavities after electropolishing is very curious, which should have a condensed oxide film on the surface [10]. The fitting result by the combined model is given in Fig. 17. The Qo-Eacc excitation curve is rather nicely fitted with H_C=505 Gauss and C=0.0323, A=1.41E-4, B=17.95, Rres=8.5 nΩ. Again, the latter three parameters were obtained from the Rs(T). As expected, in this case H_C has a rather low value. Another feature is that C is larger by one order of magnitude 10 than other results.

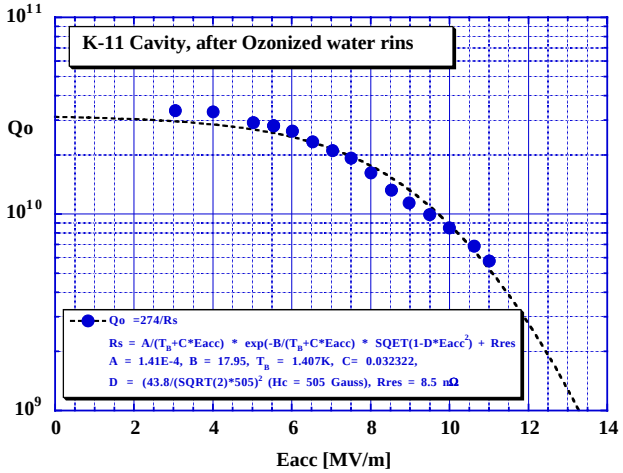

Figure 17: Analysis of the ozonated water rinsed cavity.

Nb/Cu CAVITIES

Nb/Cu Clad Cavity

By the global heating model, the temperature difference: ΔT is given as for Nb/Cu cavity case:

$$\Delta T = q\cdot\left[\frac{d(Nb)}{K_s}+\frac{1}{h_k(Nb/Cu)}+\frac{d(Cu)}{K_n(Cu)}+\frac{1}{h_k(Cu)}\right] \qquad (25).$$

In this case, the interface effect between the niobium and the copper with the Kapitza conductance and the thermal conductance of the copper are added in Eq.(13). The niobium thickness is about 0.8mm in the Nb/Cu clad cavities and is no negligible. On the other hand, the thickness of the copper is about 2.5mm. In this considered narrow temperature range, the thermal conductivity is temperature independent with copper material, and much higher (100W/(mK)). So the third term in Eq.(25) can be neglected. The Kapitza conductance of copper also larger by more than a factor 10 than niobium. Thus, ΔT can be written as:

$$\Delta T = q\cdot\left[\frac{d(Nb)}{K_s}+\frac{1}{h_k(Nb/Cu)}\right] \qquad (26).$$

From the sharp temperature dependence of Ks, ΔT should include the term: C_1*Eacc with ΔT. The second term in Eq.(26) is contributed from phonon mismatching at the Nb/Cu interface. It will be regarded as constant in this temperature range (1.2 ~ 2.2K). So the temperature increase due to this part should be proportional to $Eacc^2$. Thus, ΔT can be expressed as:

$$\Delta T = T_b + C_1 \cdot E_{acc} + C_2 \cdot E_{acc}^{\,2} \qquad (27).$$

Fig.18 is the result of temperature analysis with a Nb/Cu clad cavity, which was bonded by hot rolling [11]. In this case, both temperatures calculated from Rs(Qo(Eacc)) and heat flux increase linearly with increased Eacc. The $Eacc^2$ term in Eq.(27) is not observed. That means the Kapitza conductance of the interface between the niobium and copper is so good in case of hot roll bonding. Thus for the hot rolled bonded Nb/Cu clad cavity, Eq.16 is simple:

$$T_S = T_b + C \cdot E_{acc} \qquad (28).$$

Fig.19 is the fitting result of the Qo-Eacc excitation curve by the combined model. In this case, the cavity was electropolished and baked. The resultant fitting parameters are: A=1.71E-4, B=18.6, Rres=17.3 nΩ, C=1.30E-2, H_C=2350 Gauss. Again, the first three parameters were fixed the results by the Rs (T) temperature measurement.

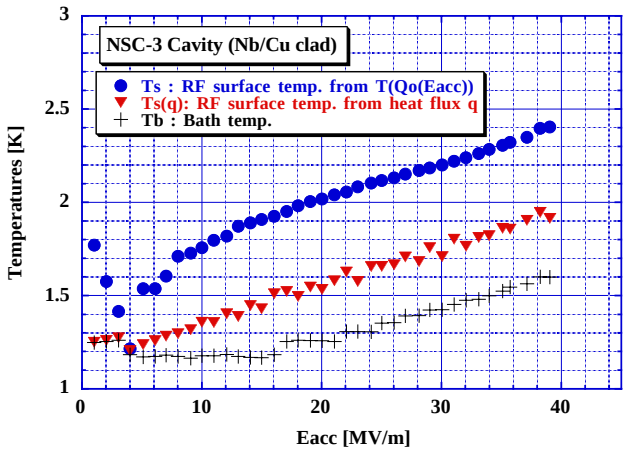

Figure 18: Temperature analysis with a Nb/Cu clad cavity.

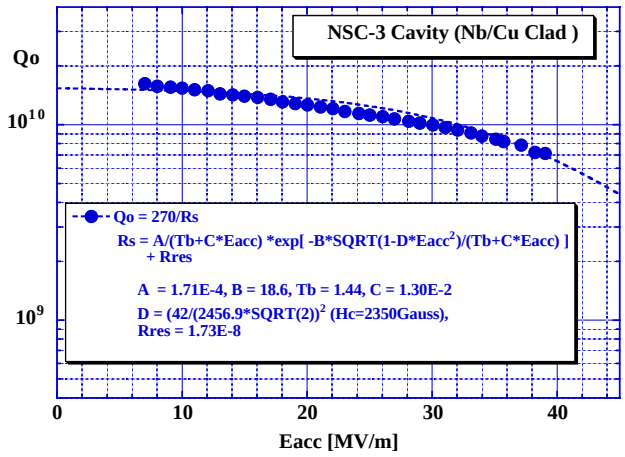

Figure 19: Qo-fitting by the combined model.

Nb Film Coated Cavity

For the Nb film coated on copper cavities, Eq.16 becomes much more simple. The thickness of niobium film is 1-2 μm and the contribution to ΔT can be negligible. Thus in this case, the contribution to ΔT is only the interface Kapitza conductance:

$$\Delta T = \frac{q}{h_k(Nb/Cu)} \qquad (29).$$

Supposing the weak temperature dependence of the h_k, ΔT should be expressed as:

$$\Delta T = C_2 \cdot E_{acc}^{\,2} \qquad (30).$$

Fig.20 is the fitting result of the Qo-Eacc excitation curve, which was measured in CERN for a niobium film coated cavity (1500MHz) [12]. The curve was fitted by the following formula. Here, A=1.94E-4 was scaled by the frequency from our 1300MHz cavity result. B was fixed our average result: 18.2. H_C, C and Rres were fitting parameters.

$$Q_o = \frac{295}{R_S},$$

$$R_S = \frac{1.94E-4}{1.7 + C \cdot E_{acc}} \cdot \exp\left[- \frac{18.2 \cdot \sqrt{1 - \left(\frac{45.5 \cdot E_{acc}}{\sqrt{2} \cdot H_C} \right)^2}}{1.7 + C \cdot E_{acc}} \right] + R_{res}$$

The resultant values of fitting parameters are Rres=0.7nΩ, C=2.00E-3, Hc=2350 Gauss. The data fitting is worse at Eacc=10 – 16 MV/m, which were neglected in the fitting. This might be due to multipacting. This fitting result suggests the steep Q-slope in the niobium film coated cavity might be in the problem of the interface Kapitza resistance between the copper and the niobium film.

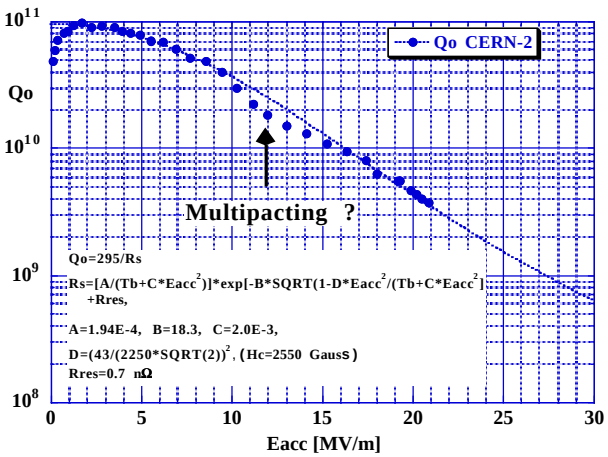

Figure 20: Qo-Eacc excitation curve fitting by the combined model for the 1500MHz niobium film coated cavity at CERN.

SUMMARIES

In this paper, we analysed Qo-Eacc excitation curves of niobium cavities by combination of two models: the global heating model and magnetic field penetration model, which is newly proposed here. This combined model can fit the curves nicely in many cases. From this analysis, several suggestive views were obtained:

1) Only the global heating model cannot explain the Q-slope III at the high gradient region.
2) There should be a hidden mechanism behind that.
3) The magnetic field penetration seems to explain the hidden mechanism, however, the assumption of the field penetration should be confirmed by the future experimental study.
4) The Q-slope III in chemically polished cavities will be related to the field enhancement due to the rough surface.
5) The oxide rich surface reduces the H_C and resulted in the Q-slope III.
6) The Nb/Cu clad bonding by hot rolling will have no problem with the interface between niobium and copper from the thermal conductance point of view.
7) While the niobium film coated cavity might be problem in the thermally poor contact at the interface between niobium film and copper substrate. The poor thermal contact might cause such a steep Q-slope.

REFERENCES

[1] P.Kneisel, Preliminary Experience with " In-situ " Baking of Niobium Cavities, Proc. of the 9th Workshop on RF Superconductivity, Santa Fe, USA, Nov. 1 – 5, 1999, pp.328 – 335.

[2] E.Kako et al., " Improvement of Cavity Performance in The Saclay/Cornell/DESY's SC Cavities ", Proc. of the 9th Workshop on RF Superconductivity, Santa Fe, USA, Nov. 1 – 5, 1999, pp.179 – 186.

[3] J.Halbritter, " Material Science of Nb RF Accelerator Cavities: Where Do We Stand 2001? ", Proc. of the 10th Workshop on Superconductivity, Tsukuba, Japan, Sep. 6 – 11, pp. 292 – 301.

[4] J.Knobloch et al., " High-Field Q Slope in Superconducting Cavities Due to Magnetic Field Enhancement at Grain Boundaries ", Proc. of 9th Workshop on RF Superconductivity, Santa Fe, USA, Nov. 1-5, 1999, pp.77-91.

[5] F.Koechlin and B.Bonin, " Parameterization of The Niobium Thermal Conductivity in The Superconducting State ", Proc. of 7th Workshop on RF Superconductivity, Gif sur Yvette, France, Oct. 17 – 20, 1995, pp.665 – 669.

[6] J.Bardeen et al., " Theory of the Thermal Conductivity of Superconductors", Phys. Rev. 113,982 (1959)

[7] P.Rhodes, "Fermi-Dirac Function of Integral Order", Proc. Roy. Soc. (London) A204, 396(1950).

[8] A.Boucheffa and M.X. Francois,"Kapitza Conductance of Niobium for Superconducting Cavities in The Temperature Range 1.6K , 2,1K", Proc. of 7th Workshop on RF Superconductivity, Gif sur Yvette, France, Oct. 17 – 20, 1995, pp.659 – 663.

[9] For example, in the textbook "Superconductivity", edited by R.D Parks, McGraw-Hill, Inc. New York, 1969, pp.150 and pp. 996.

[10] K.Asano, "Ozonized Ultrapure Water Treatment of Nb Surface for Superconducting RF Cavities", Proc. of the 9th Meeting on Ultra High Vacuum techniques for accelerators and Storage Rings, KEK, Tsukuba, Japan, March 3 – 4, 1994.

[11] I.Ito et al., "Hot Roll Bonding Method for Nb/Cu Clad Seamless SC Cavity", in this workshop, TuP40.

[12] C.Benvenuti and S.Calatroni et al., "CERN Studies on Niobium-Coated 1.5GHz Copper Cavities", Proc. of the 10th Workshop on Superconductivity, Tsukuba, Japan, Sep. 6 – 11, pp. 252 – 258.